Inter*net* Electronic Journal*

Nanociencia et Moletrónica

Junio 2014, Vol. 14, N°2, pp. 2175-2190

Electrical Characterization of PbS:Ni Nanocrystallites

L. Chaltel Lima[1•], A. Sosa Sanchez[2], María de los Ángeles Velasco[3], O. Portillo Moreno[4]

Facultad de Ciencias Químicas, Benemérita Universidad Autónoma de Puebla[1],Facultad de Ciencias de la Electrónica, Benemérita Universidad Autónoma de Puebla[2], CIDS-ICUAP, Benemérita Universidad Autónoma de Puebla[3], Facultad de Ingeniería Química de la Benemérita Universidad Autónoma de Puebla [4,] Avenida San Claudio y 18 Sur, Colonia San Manuel, Ciudad Universitaria, Puebla, Pué., 72001 México.
*Corresponding Author. Tel. (01 222) 2-29-55-00 Ext. 7519.
E-mail: leslie_chaltel92@hotmail.com

recibido: 26.03.14 publicado: 31.12.14

Citation of the article;
L. Chaltel Lima, A. Sosa Sanchez, María de los Ángeles Velasco, O. Portillo Moreno
Electrical Characterization of PbS:Ni Nanocrystallites
Internet Electron. J. Nanoc. Moletrón. 2014, Vol. 12, N° 2, pp 2175-2190

Electrical Characterization of PbS:Ni Nanocrystallites

L. Chaltel Lima[1•], A. Sosa Sanchez[2], María de los Ángeles Velasco[3], O. Portillo Moreno[4]

Facultad de Ciencias Químicas, Benemérita Universidad Autónoma de Puebla[1],Facultad de Ciencias de la Electrónica, Benemérita Universidad Autónoma de Puebla[2], CIDS-ICUAP, Benemérita Universidad Autónoma de Puebla[3], Facultad de Ingeniería Química de la Benemérita Universidad Autónoma de Puebla [4]
Avenida San Claudio y 18 Sur, Colonia San Manuel, Ciudad Universitaria, Puebla, Pué., 72001 México.
*Corresponding Author. Tel. (01 222) 2-29-55-00 Ext. 7519.
E-mail: leslie_chaltel92@hotmail.com

Abstract

Nickel doped PbS nanoparticles were synthetized in basic aqueous using by chemical bath onto glass at a deposition temperature of 40 ± 2°C. Different Ni-doping levels were obtained by changing the volume of the Ni-reagent solution into the PbS growing solution. By Transmssion Microscopy Electronic the grain size determined, was found to be ~32-5 nm range. Optical absorption spectra for the doped film in which the redshift of band gap is associated with the decrease of the grain size average. The forbidden band gap of films increased from 2.4-3.8 eV range. Ni doping of PbS is shown a conductivity 1×10^{-3} to 6.94×10^{-5} Ω range at room temperature. The activation energy for the films was determined from the slope of Dark Conductivity measurements and was estimated to be 0.15 to 0.5 eV.

Keywords: *nanocrystals, potential cell, quantum confinement effect, coordination complex, dark conductivity.*

Resumen

Nanopartículas de PbS dopadas con Ni, fueron sintetizadas en medio acuoso básico utilizando la técnica de baño químico sobre sustratos de vidrio a la temperatura de 40 ± 2°C. Diferentes niveles de Ni-Impurificante fueron obtenidos cambiando el volumen de la solución del Ni-reactivo durante el crecimiento del PbS. Mediante Microscopia Electrónica de Transmisión, el tamaño de grano fue determinado se encontró en el intervalo ~32 nm 5-3.5 nm. Los espectros de absorción para las películas PbSNi en las que el corrimiento del ancho de energía prohibida se asocia con la disminución del promedio del tamaño de grano. El ancho de banda de energía prohibida se incrementa en el intervalo 2.4 a 3.8 eV. PbS dopado con Ni es mostrada una conductividad en el intervalo de 1×10^{-3}-6.94×10^{-5} Ω a temperatura ambiente. La energía de activación fue calculada de la pendiente de mediciones de conductividad en lo oscuro y estimada en 0.15 a 0.5 eV.

1. Introduction

There has been a growing interest in the synthesis of semiconducting nanomaterials which may be conceived as polycrystalline material with lower crystallite dimension (15 nm) [1, 2, 3]. Compared to the polycrystalline material, nanomaterial possesses several properties for engineering applications. In the area of mechanical property, nanomaterials exhibit low temperature ductility, high micro hardness and yield stress [4]. Besides these, nanostructured solids have large specific heat, much higher than the bulk value and also nanomaterials show improved linear and nonlinear optical responses due to three dimensional carrier confinements [5]. Particularly, semiconductor materials in the nanostructured form offer the possibility of possessing large optical nonlinear susceptibility and ultrafast response. Nanomaterials are very attractive for realization of thermally stable and frequency selective lasers and photodetectors. The nanoestructured semiconductor materials have emerged as new materials whose properties are modulated drastically by the shape and sizes of the nanocrystallites [6]. There are, in general, a large volume of non-crystalline grain boundary (or interface) regions having short range order in the nanocrystalline thin films. This gives rise to properties different from those in the bulk having large grains with long range order. Grain boundaries are known to play in important role in explaining the properties of nanomaterials because large fractions of atoms in the materials are located within only few atomic distances of the grain boundaries. Different physical properties and specially the mechanical properties in nanostructured solids are explained in terms of these grain boundaries. But, the nature and structure of these grain boundaries are still controversial [7]. In chemical methods the growth of particles on substrates depends on dilution, pH and temperature of the chemical bath (CB) and it is also known to depend on the complexing agent used to control the growth of particles [8]. Earlier, we have reported the optical and structural properties of nanocrystalline Ni doped PbS thin solid films [9, 10] and in the present communication we present the optical and electrical properties of these films with a view to understand the carrier transport mechanism and its dependence of the sizes of the nanocrystallites. The fluctuations of the inter-grain boundary regions will also create considerable amount of disorder in the film. Effect of these disorders is reflected in the optical properties though band tailing and in electrical property thought carrier hooping at the defect states near the Fermi energy. Thus, on this frame of reference, in the present work attempt has been made to prepare PbS and Ni^{2+}-doped PbS nanostructured films by CB, in order to investigate structural, optical and electrical properties films.

2. Chemical reactions and experimental procedure

The reactions for the growth of PbS films which are doped with Ni^{2+} have been investigated by employing the cell potential values in basic media [11]. The cell potential and the Gibbs free energy are related through the Nernst equations: $\Delta G^o = - n\tau\varepsilon^o$, where *n* is the number of equivalents, τ is the Faraday constants and ε^o are the cell potential, where the ΔG^o is calculated in the reaction stage. We emphasize the importance of the formation of coordination complex $[Pb(NH_3)_4]^{2+}$, which is determinant for the release of Pb^{2+} ions and their slow recombination with S^{2-} ions under these conditions the spontaneous formations to the PbS precipitate is a controlled process [8, 9, 10]. The growth of the PbS is carried out according to the following stages: (*a*) mixing $Pb(CH_3CO_3)_2$, KOH, and NH_4NO_3, the coordination complex is generated indirectly $[Pb(NH_3)_4]^{2+}$ (*b*) The ions S^{2-} are found in the solution and are generated by the decomposition of the Tíourea in alkaline. (*c*) Therefore, to allow the slow process at surface of the substrate to take place predominantly over direct hydrolysis of Tiourea in the bulk of the reaction).] [8, 12, 13]

$$SC(NH_2)_2 + 3OH^- \Leftrightarrow CO_3^{2-} + S^{2-} + 7H^+ \quad (1)$$

$$[Pb(NH_3)_4]^{2+} + S^{2-} \Leftrightarrow PbS + 4NH_3^+$$

$$\Delta G^o = + 335.48 \text{ KJ} \quad (2)$$

$\Delta G^0 > 0$, therefore the reaction is not spontaneous.

$$Ni(OH)_2 \Leftrightarrow Ni^{2+} + OH^- \qquad \Delta G^o = + 90.71 \text{ KJ} \quad (3)$$

The reaction for the PbS:Ni^{2+}:

$$Pb^{2+} + S^{2-} + Ni(OH)_2 \Leftrightarrow PbS{:}Ni^{2+} + 2OH^-$$

$$\Delta G^o = - 29.79 \text{ KJ} \quad (4)$$

Based on the Gibbs free energy values obtained from the thermodynamic equilibrium analysis, there is large probability that the Ni^{2+} ionization states be presents in the volume of PbS, under our work conditions comparing the changes in ΔG^0, is thermodynamically probable to growth PbS:Ni^{2+}.

Preparation of polycrystalline PbS thin films on glass substrates at temperature 40°C doped with $V_{[Ni2+]}$ grown by chemical bath deposition (CBD) and pH = 11.0. The glass substrates were previously immersed in $K_2Cr_2O_7$/HCl/H_2O solution for 24 h, after

which there rinsed in deionised water and dried in a clean hot–air flow. We growth PbS films with six different levels of doping of ($V_{[Ni2+]}$) solution: 2, 4, 6, 8, 10 and 12 mLs the solutions for PbS growth in steps of two: $Pb(CH_3CO_3)_2$ (0.01 M), KOH (0.5 M), NH_4NO_3 (1.5 M) , $SC(NH_2)_2$ (0.2 M). All the solutions used were prepared with deionised water of resistivity 18.2 MΩ. The solutions were mixed and the final solution heated at 40°C for 1 h, with the substrate remaining inside the solution. The optimal volume of $V_{[Ni2+]}$ $Ni(NO_3)_2$ (0.023 M). Was determined after several trials, until films had good adherence. This solution is routinely added to the mixture of the reaction during the growth of the PbS film. The samples were labelled PbS0 for the undoped sample and PbSNi2,..,PbSNi12 for the doped samples. The total volume of the growing-solution consists of the volume-solution (V_{PbS}) for the PbS growth plus the volume-solution $V_{[Ni2+]}$ containing the doping Ni^{2+} chemical agent: $V_{PbS} + V_{[Ni2+]} = V_{tot}$. The colour of the chemical bath changed from a colourless and transparent solution to a black and turbid one in less than 20 min. The films were silver colour, homogeneous, polycrystalline reflective and with good adhesion to the substrate. Transmission Electronic Microscopy measurements carried out using an H-7500 model (Hitachi Ltd., Tokyo, Japan).The optical absorption spectra, measured employing a Varian Cary 100 Spectrometer over the 350-3200 nm wavelength range with an accuracy of Δλ =±0.5, allowed to calculate the forbidden band gap energy (E_g) by using the $(\alpha hv)^2$ vs. energy plot, where α is the optical absorption coefficient and *hv* the photon energy. Dark conductivity measurements as function of absolute temperature over the 300-600 K range were achieved by using a closed to a vacuum system with a pressure of 10^{-2} mbar. A Keithey 617 programmable electrometer with accuracy of Δl =±0.005 pA, ΔV=±0.0025 V, and DL4600 deep level transient spectrometer with an accuracy of ΔT =±0.05 K were employed for sheet resistivity measurements.

3. Results and discussion

The Figure 1 displayed a typical electron dispersion spectroscopy (EDS) pattern and details of a relative analysis for (*a*) undoped (*b*) doped-PbS. The elemental analysis was performed only for Pb, S and Ni, deriving the average atomic percentage of undoped and doped Pb/S. The semi-quantitative measurements of atomic concentration of elements were achieved by EDAX analysis of the films was carried out by using the SEM technique for undoped and doped PbS thin films at different points to study the stoichiometry of the films.

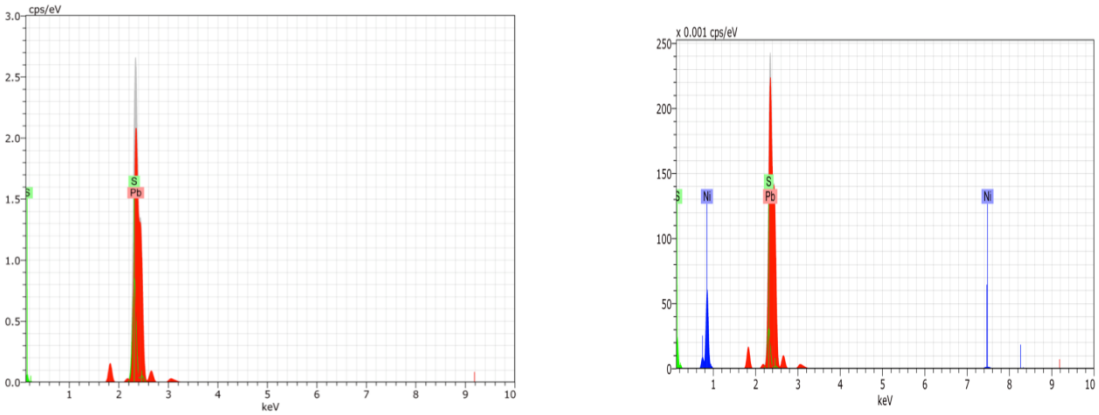

Figure 1. EDAX patterns (*a*) undoped-PbS0Ni, (*b*) doped-PbS12Ni, with 12 mLs.

In Table I are displayed the atomic concentrations of Pb, S and Ni. For the samples the increase in concentration of Ni in PbS films is easily noted, reaching a percent value of Ni = 11.51.

	Atomic concentrations		
Sample	Pb	S	Ni
PbS-Ni0	56.35	43.05	0.0
PbS-Ni6	70.10	18.38	11.51
PbS-Ni12	56.29	33.49	10.22

Table I. The atomic concentrations of Pb, S and Ni..

The crystal structure of the PbS undoped and doped films has been studied by Transmssion Microscopy Electronic (TEM). A typical bright plan view obtained image of the nanoparticle PbS films is show in Fig. 1. Scale bar 20 nm (*a*) Undoped-PbSNi0, (*b*) Doped-PbSNi6 (with 6 mLs). (*c*) Doped-PbSNi12 (with 12 mLs). The micrographs of the films with doping levels of $V_{[Ni2+]}$: 2, 4, 8 and 10 mLs are not shown.

Such results revealed that small particles attach together with a common crystallographic orientation, and most of the produced crystals have irregular shapes. The sizes of the clusters are mostly 3.5-5 nm. The micrographs with an electron beam direction close to (111) zone axis in strongly under focused condition and as such, the black/gray contrast in white background represents the PbS nanoparticle in the range 3.5-5 nm. The average grain size (GS) in the films is observed to decrease while doping is increasing. These results are in concurrence as evidenced from x-ray diffraction reported [14]. Selected-area electron diffraction (SAED) pattern of plain core (PbS) and

core-shell nanocrystals is displayed. The sharp rings presented in SAED patterns are indicative of polycrystalline nature of the films. The SAED patterns were analyzed using the standard procedure. The SAED pattern with clear spots indicates perfect orientation around (111) plane. The blurring of the diffraction ring in the SAED pattern of core-shell nanocrystals in comparison to that of plain core structures revealed the deposited nanoparticle thin films. From this measurement, it is clear that both undoped and doped films are polycrystalline in nature.

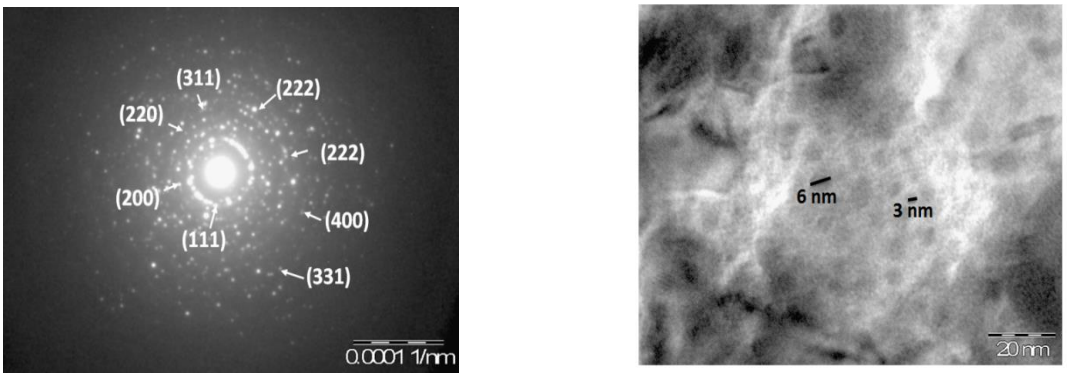

(a)

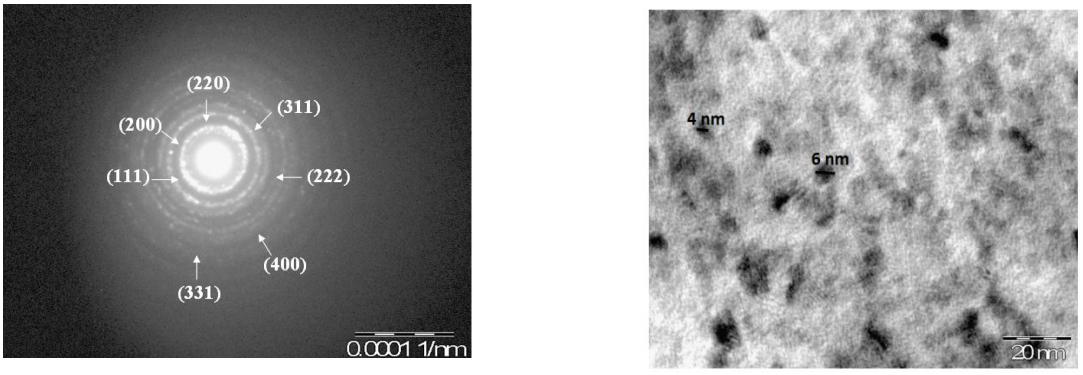

(b)

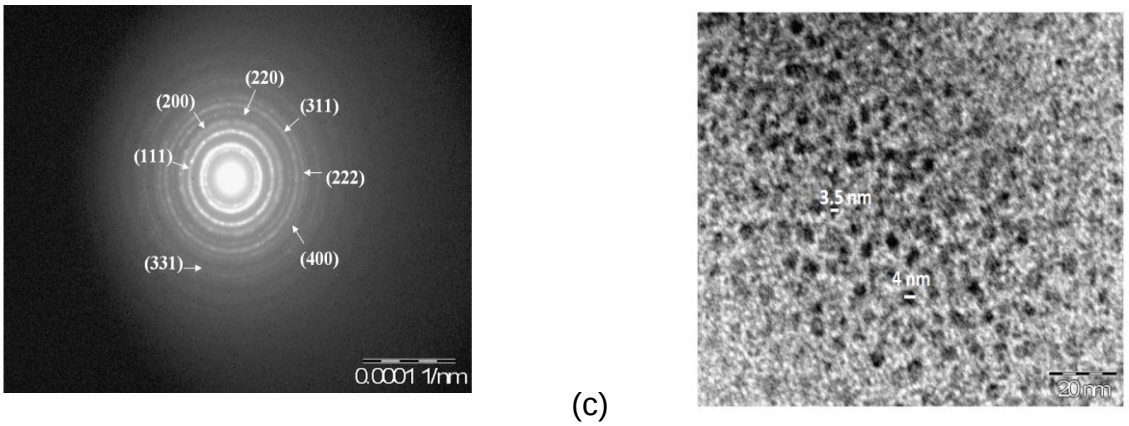

Figure 2. TEM images of nanocrystals: (*a*) Undoped-PbSNi0 (*b*) Doped-PbSNi6 (with 6 mLs). (*c*) y (*d*) An HRTEM of PbSNi12 and their respective selected area electron diffraction (SAED) pattern of plain core (PbS) and core-shell nanocrystals.

The optical absorption of PbSNi thin films was studied in the wavelength range 350-3200 nm. The variation optical coefficient with wavelength was further analysed to find out the nature of the electronic transition across the optical forbidden band gap (E_g). The nature of the transition was determined using the relation

$$(\alpha h\nu) = A\left(h\nu - E_g\right)^n \qquad (5)$$

where *A* is a constant and *hv* is the energy of photon and *n* = 1/2 for allowed direct transition. The value of absorption coefficient is found to be the order to 10^4 cm^{-1} for all composition that supports the direct E_g nature semiconductor. Fig. 3 shows a graph of E_g vs. $V_{[Ni2+]}$ and in the inferior right part the plot shows the absorption spectrum for the sample PbSNi6. In this plot, it can be observed a E_g = 3.8 eV value for the PbSNi6 sample, through the intersection of the straight line with the axis of the photon energy, an E_g value is obtained in a similar way to all samples. Those results are very similar of the reported data of other PbS nanostructures [15, 16].

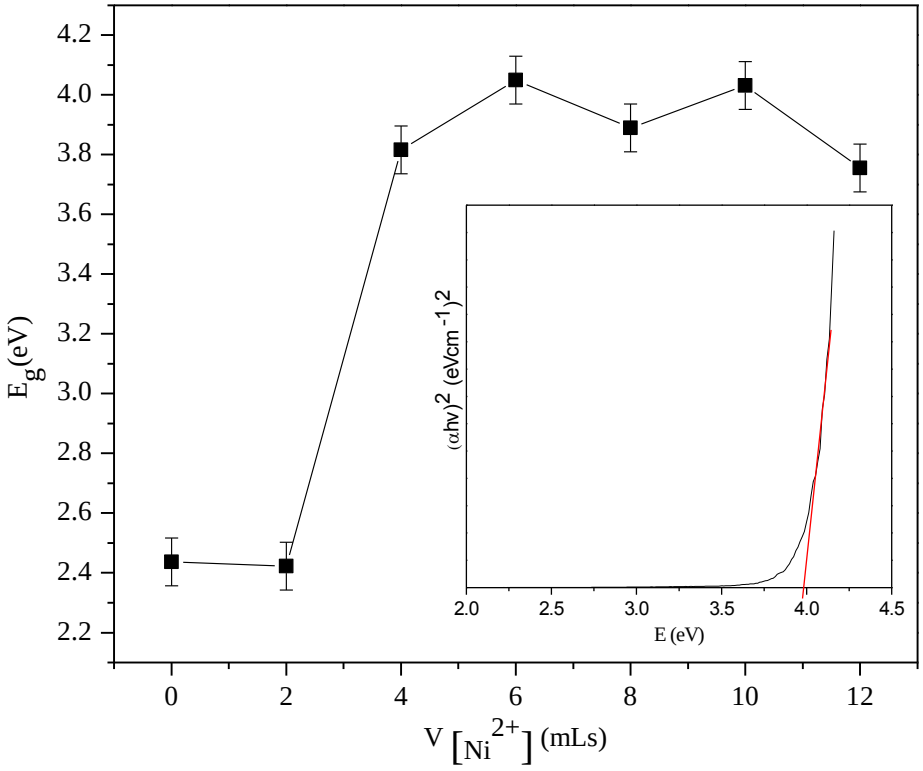

Figure 3. The band gap energy (E_g) as function of $V_{[Ni2+]}$. The inset illustrates the method to calculate E_g from optical absorption measurements.

The confinement effect appears as a shift in edge of the absorption spectra and the absorption to lower wavelengths, possibly due to the decrease in grain size (GS), the decrease in number of defects. The experimentally observed E_g values for the shift indicated an alloying between nanocrystalline PbS films. Such increase has been reported [16, 17]. The E_g for undoped and doped layers in the 2.4-3.8 eV range the large experimentally observed E_g in the nanoparticle films for bulk shows the extent of quantum size effect in the nanoparticle films. The fundamental optical transition of PbS films (E_g = 0.41 eV) is not observed in these films, presumably because of complete mixing of PbS with Ni^{2+} affording an unique ternary intermetallic compound of the $Pb_xNi_{1-x}S$ type [14]. It is observed that the size effect on the optical band gap is stronger in nanoparticle films than in PbS nanoparticle of 12-17 nm (average crystallite size) and show an E_g: 2.15-1.95 eV respectively [18]. The observed increase in the quantum size effect could possibly be attributed to a decrease in the effective mass [19]. The increased in E_g when increasing of $V_{[Ni2+]}$ in the films is reflected by the presence of an excitonic structure material. Excitonic structures are readily observed in large E_g

semiconductors with binding energy such as CdSe [20]. A shift has been observed in the position of the excitonic peak towards higher energies in CdSe crystallites has been explained due to a decrease in crystallite size [20]. The redshift of the E_g is associated with the decline of the SG. It has been reported that the kinetic energy of phoelectrons emitted from core levels decreases with decreasing of the nanocrystals size. This phenomenon is called the size shift. The size shift values the same for donator and acceptor in the compound [21].

The electrical resistivity (σ) of PbSNi thin films was measured using a dark conductivity (DC) two-probe method in air in the temperature 300-600 K range. Fig. 4 represents the variation of the logarithm of conductivity (lnσ) with the reciprocal of temperature (1/kT) for PbSNi films. It is observed that the conductivity of the films decrease with increases $V_{[Ni2+]}$, indicating the semiconducting nature of the of the films. Such increase has been reported [22]. The conductivity decreased with $V_{[Ni2+]}$ showing typical Arrhenius type of energy of activation [23]

$$\sigma = \sigma_0 e^{-\frac{E_a}{kT}} \quad (6)$$

where E_a is the activation energy, *k* Boltzmann constant. The lnσ versus 1/*kT* and two activation energies may be obtained from these two temperatures zones. The vertical dotted line in Fig. 4 points out lnσ values at 1/kT. They very low value indicated that the hooping transport may dominate in these highly disorder films as result of hopping of the carriers between localized states within or outside the coulomb gap. This change in conductivity may be attributed to change in the density of free electrons an change in mechanism of scattering at the surface of nanostructured films due to grain boundaries. If we consider a disordered system in which the electronic states close to the Fermi level are localized, the electron-electron interaction would reduce the density of states in the vicinity of the Fermi level [24].

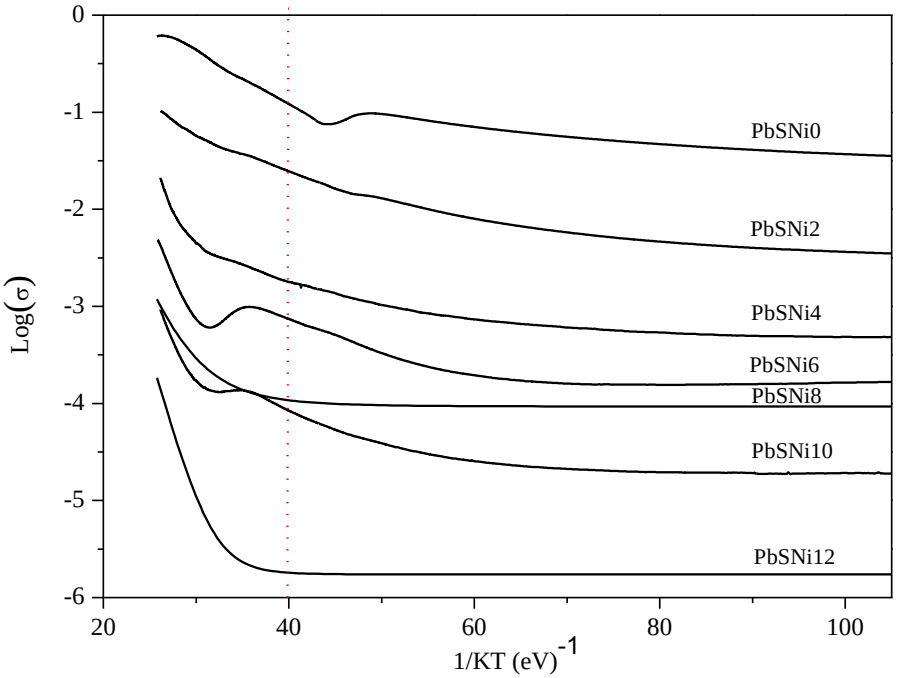

Figure 4. logσ as function of T^{-1}, in the temperature range for doped-PbS films.

In this case PbS0 thin films, indicating the predominance of extrinsic (impurity) conduction process due to presence of Pb^{2+} vacancies formed during the deposition of the films [23]. At further higher temperatures, E_a for PbSNi decreases further with increases $V_{[Ni2+]}$. [25]. This may be attributed to the increase in E_g due the incorporation of Ni^{2+}, which acts a donor level below the conduction band (forbidden gap) and decreases the electrical resistivity of PbSNi layers. The electrical conduction mechanism in polycrystalline semiconductors is vastly influenced by inherent intercrystalline boundaries. These grain boundaries regions are dominated by network of dislocations which are accompanied by large strain fields. Like grain boundaries, these locations also act as scattering centres for the charge carriers [26]. Although accurate modelling is a very difficult task, several models exist where, inside the crystallite, a series of distinct high conductivity (bulk) and low conductivity (grain boundary) regions are considered [27]. As can be seen from the room temperature conductivities PbSNi films and crystal sizes (Figure 2), there is significant correspondence between the size and the conductivity of undoped-PbS0 and doped-PbSNi as suggested by these models. However, when the carrier concentration also changes for these compound semiconductors, the overall change in conductivity has attributed to both cases. Therefore, a linear dependence between size and conductivity cannot be expected

as the generation of charge carriers is affected by the lattice defect which vary strongly within this group of samples. Fig. 5 shows the plot of activation energies (E_a) vs. $V_{[Ni2+]}$ for undoped PbS0 and doped PbSNi films. The gradual decrease in E_a with a decrease in temperature suggests that the conduction is by hopping of carriers among localized states [22]. The inset of Fig. 5 displays logσ vs. $V_{[Ni2+]}$. The observed difference in the conductivity of the doped films can be ascribed to the increase in the high barrier between PbSNi nanocrystals. It must be noted that the decrease of E_a and diminution of conductivity in doped layers can be related to a stronger compensation of the Ni^{2+} donor and, in this regard, we deem that the high resistance of the nanocrystalline films is due to small crystallite sizes. Change in crystallite size will mainly affect the mobility of the carriers and therefore change the resistance.

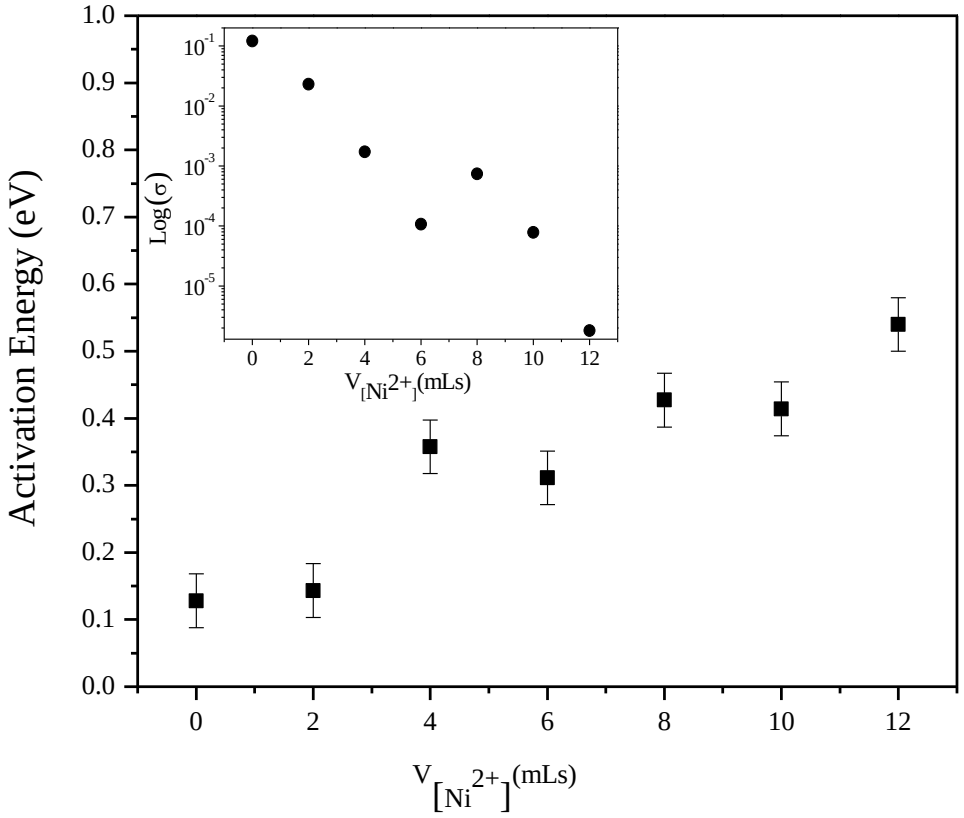

Figure 5. Activation energies (E_a) vs. $V_{[Ni2+]}$ for undoped- and doped-PbS films. The inset exhibits E_g vs. $V_{[Ni2+]}$.

E_a for films was calculated from the slope of log σ curve vs. temperature. This energy was estimated to be 0.15 to 0.5 eV. For PbS films, two sensitizing centres were

established with E_a values of approximately 0.13 and 0.22 eV. Fig. 6 shows the plot of activation energies E_a vs. grain size (GS) for undoped and doped thin films, the GS has been reported in previously work [14]. The linear nature of E_a attributes the presence of the decrease of defect levels films. It is observed that the room temperature E_a decrease continuously with increase in $V_{[Ni2+]}$. This decrease in E_a can be attributed to decrease in grain size and quantum confinement.

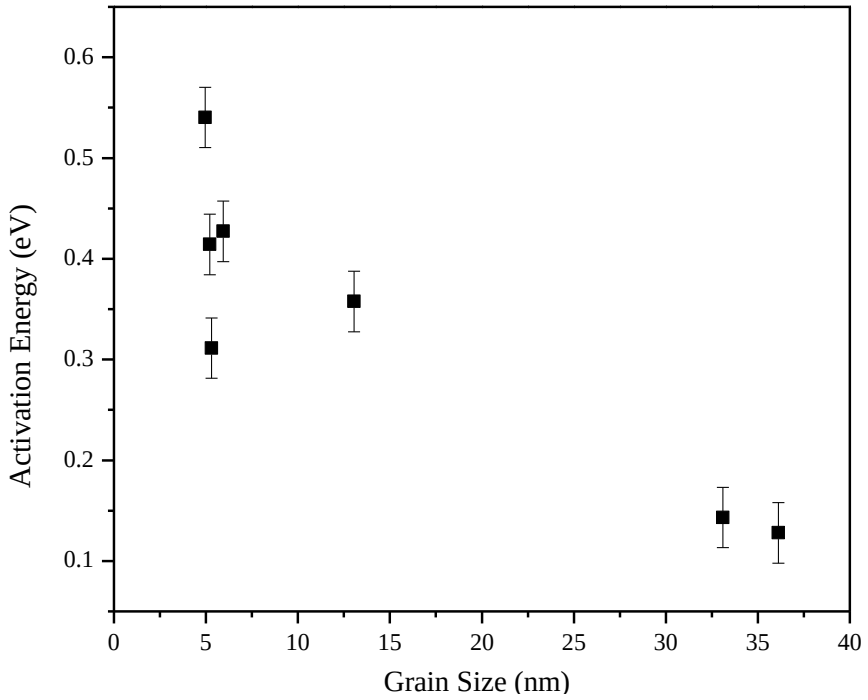

Figure 6. Activation energies vs. grain size for PbSNi films.

.

Recently, percolation methods were developed based on potential fluctuation due to intercrystalline barriers. Neither of these models can explain all the experimental features of PbS0 and PbSNi films, but showed that the structural properties play a decisive role in conductivity of the chemically deposited films. As a result of earlier investigations, it was found that there is an optimum grain size in PbSNi films, for which the conductivity signal reaches a maximum and minimum. While the single semiconductors quantum dot is relatively well understand, the understanding of the physical properties of dense ensembles of quantum dots is still at a rudimentary level. In particular, while considerable advances in the evaluation of the optical properties and in the interdot conduction mechanics in such ensembles have been reported, correlation was made between their macroscopic, disorder-semiconductor like transport and

phototransport properties, the confinement induced level shifts in the corresponding individual nanocrystallites. However we have previously reported that crystallite-size dependence of the transport and phototransport properties in solid-state ensembles of semiconductor quantum dots by finding a Meyer-Neldel-like behaviour for the former and by comparing the experimental results with computer simulations for the latter-showed that the aforementioned evidences were associated with the quantum confined induced variation of the E_g in the individual dots [28].

Conclusions

We have reported the growth of undoped PbS0 and doped-PbSNi affording nanocrystalline films by CB technique. TEM image for nanoparticle films of the PbS0 and PbSNi were obtained, the micrographs with an electron beam direction close (111) zone axis in strongly under focused condition with nanoparticle in the range 3.5-5 nm. Optical absorption spectra are quantified for the PbSNi film in which the redshift of band gap is associated with the decrease of the average TG. The E_g of films increased from 2.4-3.8 eV when doping $V_{[Ni2+]}$ is increased. The thermal E_a for films was determined from the slope of log σ curve versus temperature. This energy was estimated to be 0.15 to 0.5 eV.

References

[1] Ruby Chauhan, Ashavani Kumar, Ram Pal Chaundhary, *Appl. Surf. Sci.* **270** (2013) 655.
[2] Fifei Pang, Xioaolan Sun, Hairum Guo, Jiwen Yan, Jin Wang, Xianglong Zeng, and Zhenyi Chen, Tingyum Wang, *Optics Express* **18** (2010) 14024.
[3] S. M. Slim, O. Hamid, *Renewable Energy* **24** (2001) 575.
[4] R. Lozada Morales, O. Portillo Moreno, S. A. Tomas, O. Zelaya Ángel, *Optical Materials* **35** (2013) 1023.
[5] Dario Ruso, Paolo Falcaro, Stefano Costacurta, Massimo Gugliemi and Alessandro Martuchi, *Chem. Matter* **17** (2005) 4965.
[6] Mausod Salvati-Niasari, Azham Sobhani, Fatemeh Davar, *J. of Alloys Compounds* **507** (2010) 77.
[7] N. Wang, Z. Wang, K. T. Aust, U Erb, *Acta Metallurgica et Materialia* **43** (1955) 519.
[8] O. Portillo Moreno, H. Lima, V. Ramírez Falcón, J. Martínez Juárez, G. Juárez Díaz, R. Lozada Morales, B. Rebollo Plata, R. Palomino, A. B. Soto, O. Zelaya Ángel, *J. of Electrochem. Soc.* **153** (2006) 926.

[9] H. Lima Lima, C. Aguilar Galicia, A. Camacho Yañez, M. Hernández Hernández, M. Zamora Tototzintle, K. Barrios Henandez, L. A. Chaltel Lima, Rl Lozada Morales,, O. Zelaya Angel, O. Portillo Moreno, *Revista Naturaleza y Tecnologia* **1** (2013) 4.

[10] S. Rosas Castilla, M. Zamora Tototzintle, R. B. López Flores, L. Chaltel Lima and O. Portillo Moreno, *J. of Materials Science and Engineering* ***A*** **3** (2013) 305.

[11] J. Bethune and N. A. S. Loud, *in Standard Aqueous Potential an Temperature Coefficients at* 25°C, C. C. Hampel, Skokie, II. (1969).

[12] R. Gutiérrez Pérez, G. Hernández Téllez, U. Peña Rosas, A. Moran Torres, J. Hernández Tecorralco, L. Chaltel Lima, and O. Portillo Moreno, *J. of Materials Science and Engineering A* **3** (2013)1-13.

[13] R. Palomino Merino, O. Portillo Moreno, L. A. Chaltel Lima, R. Gutierrez Perez, M. De Icaza Herrera, V. M. Castaño, *J. of Nanomaterials* ID 507647 (2013).

[14] O. Portillo Moreno, L. A. Chaltel Lima, M. Chávez Portillo, S. Rosas Castilla, M. Zamora Tototzintle, G. Abarca Ávila, R. Gutiérrez Pérez, *ISRN Nanotechnology* ID 546027.

[15] Chunguang Li, Ying Zhao, Feifei Li, Zhan Shi and Shounhua Feng, *Chem. Mater.* **22** (2010) 1901.

[16] Nidhi Mathur, Rakesh K. Joshi, G. V. Subbaraju, H. K. Shegal, Physica **E 23** (2004) 56.

[17] Rakesh K. Joshi, *Solid state comm.* **139** (2006) 201.

[18] Rakesh K. Joshi, Aloke Kanjilal, H. K. Shegal, *Appl. Surf. Sci.* **221** (2004) 43.

[19] S. Jana, R. Tapa, R. Mayty, K. K. Chattopadhyay, *Physica E* **40** (2008) 3121.

[20] Rivera Márquez, M. Rubín Falfán, R. Lozada Morales, O. Portillo Moreno, O. Zelaya Ángel, J. Luyo Alvarado, M. Meléndez Lira, L. Baños López, *phys. stat. sol.* **188** (2001) 1059.

[21] Kovalev, D. Wainstein, A. Rashkovskliv, O. Osherov, Y. Golan, N. Ashkenasy, *Vacuum* **86** (2012) 638.

[22] Rakesh K. Joshi, H. K. Shegal, *Physica* ***E*** **23** (2004) 168.

[23] J. Dávila Pintle, R. Lozada Morales,, M. R. Palomino Merino J. A. Rivera Márquez, O. Portillo Moreno, O. Zelaya Ángel, *J. Appl. Phys.* **101** (2007) 013712-1.

[24] S. K. Mandal, S. Chaudhuri, A. K. Pal, *Nanostructured Materials* **10** (1998) 607.

[25] R. Lozada Morales, M. Rubín Falfán, O. Portillo Moreno, J. Pérez Álvarez, R. Hoyos Cabrera, M. C. Avelino Flores, O. Zelaya Ángel, O. Guzmán Mandujano, P. del Ángel, J. L. Martínez, L. Baños López, *J. of Electrochem. Soc.* **146** (1999) 2546.

[26] Paulomi Roy, Sunneel Kumar Srivastava, *J. Phys. Appl. Phys.* **39** (2006) 4771.

[27] J. I. Pankove, *Optical processes in Semiconductors*, Englewood Chiffs. N J Prentice Hall (1971).

[28] Balberg, E. Shavir, Y. Dover, O. Portillo Moreno, R. Lozada Morales, O. Zelaya Angel, *Physical Review B* **75** (20007) 153301-1.